Data Transformation for Super-Resolution on Ocean Remote Sensing Images

Yuting Yang, Kin-Man Lam, Xin Sun, Junyu Dong, Muwei Jian, Hanjiang Luo

Data Transformation for Super-Resolution on Ocean Remote Sensing Images

Yuting Yang[1,2,3], Kin-Man Lam[2], Xin Sun[3], Junyu Dong[3,4,5], Muwei Jian[6], and Hanjiang Luo[1]

[1] Shandong University of Science and Technology, Qingdao 266590, China
[2] Department of Electronic and Information Engineering, The Hong Kong Polytechnic University, Hong Kong 999077, China
enkmlam@polyu.edu.hk
[3] Department of Information Science and Engineering, Ocean University of China, Qingdao 266100, China
sunxin1984@ieee.org;dongjunyu@ouc.edu.cn
[4] Haide College, Ocean University of China, Qingdao 266100, China
[5] Institute of Advanced Ocean Study, Ocean University of China, Qingdao 266100, China
[6] School of Computer Science and Technology, Shandong University of Finance and Economics, 7366 Li Xia, Jinan, China 250000

Abstract. High-resolution ocean remote sensing imaging is of vital importance for research in the field of ocean remote sensing. However, the available ocean remote sensing images are often averaged data, whose resolution is lower than the instant remote sensing images. In this paper, we propose a data transformation method to process remote sensing images in different locations and resolutions. We target satellite-derived sea surface temperature (SST) images as a specific case-study. In detail, we use a modified very deep super-resolution (VDSR) model as our baseline model and propose a data transformation method to improve the robustness of the model. Furthermore, we also illustrates how the degree of difference in the data distribution influences the model's robustness and also, how our proposed data transformation method can improve the model's robustness. Experiment results prove that our method is effective and our model is robust.

Keywords: Deep learning · super-resolution · sea surface temperature · data transformation · ocean-front.

1 Introduction

Sea surface features are an important factor in oceanography and can be applied to many fields, such as air-sea interaction, severe weather prediction, ocean engineering, etc. The sea surface features include, but are not limited to, sea surface temperature, sea surface chlorophyll, and sea surface height. It has been a popular topic for many years, bringing together a large amount of remote sensing sea surface feature data with different resolutions, thus allowing for new insights

in small-scale processes at a larger-scale area coverage. Based on these feature images, we can further research some important marine environmental characteristics, such as vortex, ocean-fronts, etc. However, research on sea surface features is limited by the resolution of the weekly, or monthly, averaged remote sensing images, and the cloud contamination of the instant remote sensing images. Thus, how to increase the resolution of remote sensing images and eliminate the cloud contamination are of great valuable for various ocean-related research works.

In this paper, we take one of the most famous marine environmental characteristics, named ocean-front as a specific case-study to analyze the effectiveness of our super-resolution method and data transformation method. Ocean-front is one of the most well-studied ocean mesoscale characteristics. It is usually expressed as open streamline in high-resolution remote sensing images that separates water masses with different physical properties, for example, water masses that contain distinct amount of salt, heat, and chemicals. It can be transported by currents, and mix with surrounding water masses. Usually, jets and strong currents will engender ocean-front, and the existence of ocean-front makes it difficult for particles to cross. Thus, the water masses separated by long-living ocean-fronts could maintain its biogeochemical properties for a long time. They stand a show of becoming the best living environments for various kinds of fish species and forming into a complicated ecological system.

There are mainly two kinds of ocean-front detection methods, one is a data analysis method based on the physical characteristics of ocean-front images [1, 2], and the other one is a data-learning method based on the mapping relationship between the input and the ground-truth images [3, 4]. In our research, we use one of the state-of-the-art ocean-front detection methods, named Microcanonical Multiscale Formalism (MMF), to detect ocean fronts. The method has been used to extract ocean fronts in sea surface temperature (SST) images in our former work [5–7]. Under the microcanonical framework, the algorithm analyzes the critical transitions in oceanographic satellite data by calculating the Singularity Exponents (SE), and transforms SST images into clean and simple line drawings of ocean fronts. The method has been validated by oceanographers and has an advantage over traditional edge extraction methods in dealing with satellite oceanographic images [8].

In this paper, we focus on the super-resolution of remote sensing SST images, in consideration of the noise caused by clouds. The state-of-the-art super-resolution methods can be roughly divided into two categories. One is the traditional method based on EOF or analog schemes, and the other one is the data-driven approach, such as neural networks and machine learning methods. Ducournau et al. [9] were the first to apply super-resolution methods, based on the super-resolution convolutional neural network (SRCNN) proposed in [10], to SST images. The experiment results showed an obvious improvement of the super-resolution performance based on a convolutional network, compared to those traditional methods. However, shallow convolutional networks have been surpassed by deep neural networks in many tasks. Deep neural network is a key breakthrough in the field of computer vision and pattern recognition. For

the past decade, deep networks have enabled machines to classify images with accuracy as high as humans can. The most important breakthrough is "residuals learning", which can reconstruct the learning process and redirect the flow of information in deep neural networks effectively. It improves the performance of deep neural network without increasing the computing cost. For this reason, the Very Deep Super-Resolution network (VDSR) proposed in [11], is employed as our baseline model. We improve its performance by enhancing its ability to integrate low-level features with high-level features. VDSR is a deep learning approach proposed for image super-resolution. It has 20 convolutional layers, which is much deeper than SRCNN, which contains 3 convolutional layers only. The modified VDSR network proposed in our previous work [6] can help us to reconstruct high-resolution images with high quality from low-resolution ones. The Enhanced Deep Super-Resolution network (EDSR) proposed in [12], is a more complex and deeper residual network, compared with VDSR, whose performance on low-resolution images, for example, the Set5 database proposed in [13], is better than that of the VDSR model. In this paper, we compare the performance of these two deep neural networks with the modified VDSR model for SST images.

The rest of this paper is organized as follows. In the second section, we propose our data transformation method. We introduce the databases used in our experiments in Section 3. A detailed description on the experimental setup and evaluation methods is given in Section 4. In Section 5, we analysis the experiment results. Then, we conclude this paper and give our future research plan in Section 6.

2 Data Transformation

Unlike standard images, whose pixel values range from 0 to 255, SST images typically range from 0 to 5000. Consequently, the VDSR and EDSR networks cannot process remote sensing or SST images directly. As the dynamic range of SST images is more than 10 times that of standard image, this makes it difficult to use existing deep neural networks to learn the mapping between the input and the ground-truth data.

200	220	330
200	50	10
340	50	100

0	20	30
0	50	10
40	50	0

Fig. 1. The effect of data transformation. The input image is shown on the left, while the processed image is displayed on the right. We set the data domain within [0 - 100]. Then, the data domain of the input image is transferred from [0 - 340] to [0 - 100].

Data transformation is to transfer the data domain from one to another. The deep neural network trained on one data domain can hardly be adapted to another data domain. The data transformation method can solve the domain adaptation problem. The effect of the method is shown in Figure 1.

Before feeding SST images into EDSR and VDSR, their data domain has to be compressed. The common compression operation can blur the SST images. In this situation, even though the network is deep and its structure is well designed, it is still a great challenge to reconstruct high-resolution image from the blurred SST image. We trained and tested EDSR and VDSR on the compressed images from the ocean SST database. The experimental results show that the network fails to improve the resolution of the SST images.

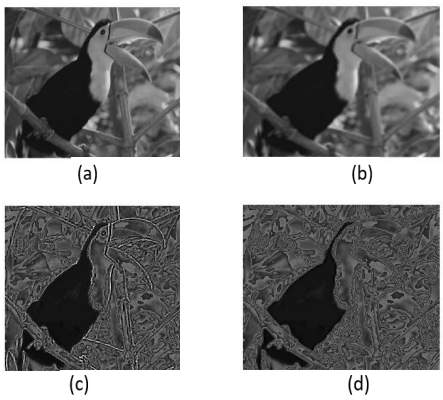

Fig. 2. The effect of data transformation on the Set5 database. (a) The y channel of a ground-truth image (data domain 0-255), (b) the y channel of the bicubic image (data domain 0-255), (c) the transformed ground-truth image, with data domain [0-100], and (d) the transformed bicubic image, with data domain [0-100].

To improve the performance, we propose a data transformation method, which transforms the SST data from one domain to another, while the data is not blurred. In order to verify the impact of the data transformation method, we trained and tested EDSR and VDSR on the transformed data from the low-resolution and high-resolution ocean SST databases. The experiment results proved the effectiveness of the proposed method. Moreover, to evaluate the robustness of the data transformation method, we also applied the same data transformation method to the 291 database. Then, we trained VDSR on the 291 database, but tested it on Set5. The experiment results proved that the data transformation method is robust.

As shown in Figure 2, we transform the data domain of the bicubic interpolation image to $0 - 100$. We also apply the same operation to the ground-truth images. In this way, we can keep the difference between the input image and the

ground-truth image unchanged, so as to maintain the data dependence of the input and the ground-truth images. Transforming the data domain also makes the difference between the ground-truth and bicubic images more obvious. According to the experiments, the best data domain for standard images to be transformed is from the domain $0-50$ to the domain $0-150$, larger or smaller will make the performance worse.

Figure 3 presents a SST image before and after the transformation. The ground-truth image is chosen from the low-resolution ocean SST database. Similarly, the SST image can maintain its dependence between data after the data domain transformation. According to experiments, the best data domain that the original database can be transformed is from the domain $0-5$ to the domain of $0-250$, larger or smaller makes the performance worse.

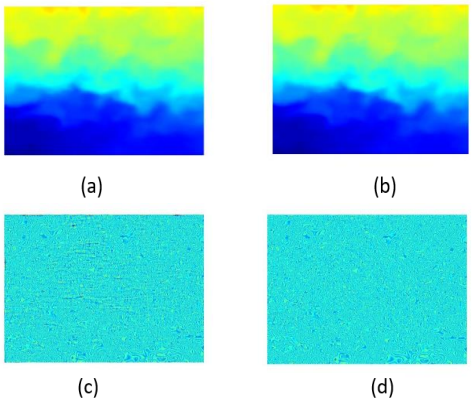

Fig. 3. The effect of data transformation on the Ocean SST database. (a) The ground-truth image (data domain 0-3000) (b) the bicubic image (data domain 0-3000) (c) the transformed ground-truth image (data domain 0-5) and (d) the transformed bicubic image (data domain 0-5)

3 Databases

In this work, we compare the difference in data distribution between standard and remote sensing images. Specifically, we use the 291 database as a case-study for standard images and the China Ocean SST database for remote sensing images.

As well, we also used another four databases for comparison and evaluation, including the Ocean SST database, the High-resolution Ocean SST database, the Low-resolution Ocean SST database and the SST Ocean-Front database. We propose the Ocean SST database, the high-resolution and low-resolution ocean SST databases, for comparing the performance of different methods on coastal

and ocean areas in high-resolution and low-resolution SST images. Furthermore, we also propose a SST ocean-front database to evaluate the performance of different models on the SST ocean-front super-resolution task. In the following, we will introduce these databases in detail.

The China Ocean SST database: This database is proposed in our previous paper [1]. This database contains a total of 600 daily-averaged AVHRR SST images, covering China's coastal waters (112.5E-135E,10N-40N) with a spatial resolution of 5 km approximately. The waters considered in the database are highly dynamic, and contains complex turbulence structures. This is because the waters are in a part of the Kuroshio Current system, which can convey a great amount of mass and power, such as heat, from low-latitude to mid-latitude waters [14]. In this paper, we consider the time series from January to April, between 2007 and 2011 as the training data, and the time-series from January to April, in 2012 as the evaluation data.

The High-resolution Ocean SST database: This database contains 150 images, captured from 1st January 2011 to 30st May 2011. This database covers the intersection waters (155E-180E, 30N-50N), where the Kuroshio, Oyashio and North Pacific warm currents cross. These currents have great implications on the global climate and marine fisheries [14, 15]. Image super-resolution in these areas may increase the prediction accuracy on marine climate change, give a better guidance for the marine fishing industry, and prevent the occurrence of marine disasters.

The Low-resolution Ocean SST database: This database corresponds to the low-resolution counterpart of the High-resolution Ocean SST database, so it covers the same waters, with a downsampling factor of 5. This database is used for comparison with the high-resolution database.

The Ocean SST database: This database contains 1500 SST images, captured from January 2008 to December 2011. Each pixel in the image represents an area with a spatial resolution of 5km approximately. The database covers the intersection waters (155E-180E, 30N-50N), where the Kuroshio, Oyashio and North Pacific warm currents cross. This database is used to evaluate the performance of different methods.

The SST Ocean-Front database: This database consists of ocean-front images processed by the MMF method, on the Ocean SST database. This database is also used for the performance evaluation of different methods.

Before training and testing the networks, all the data in the databases are processed using the data transformation method. All the output data are also processed by our data transformation method, before evaluating the performance.

4 Experimental Setup and Evaluation Methods

The data domain difference between the databases often make a deep model trained on one database unable to achieve satisfactory performance on another database. Thus, the domain adaptation problem is a great challenge for training a robust deep model, and this problem inspires our research. On the one hand,

we want to know whether or not the data domain difference between the two databases can influence the model performance and the degree. On the other hand, we need to identify which properties of the data contribute most to the difference.

Besides, deeper networks usually gain better performance. Since EDSR is deeper than VDSR, we want to know whether or not EDSR can achieve better performance than VDSR.

Furthermore, since the ocean-front is one of the most important factors in ocean biogeochemical environment, can we upsample the ocean-front images directly?

4.1 Experimental Setup

We compare the VDSR model trained on the 291 database to the same model trained on SST databases. We aim at evaluating whether or not the data-distribution difference between these two database will influence the model performance and the degree. Then, we can gain an insight into the robustness of the VDSR model for databases with different data distribution. This suggests that we can design more effective experiments. Thereby, we further compare the performance of VDSR and the modified VDSR model, so as to figure out which model is more robust.

In another aspect, since the domain adaptation problem exists, we intend to find out what makes the difference. More specifically, we aim to find out which part of the data contributes most to the difference. Through careful analysis on the SST data and the natural image data, we can have a general guess that the coastal waters is the key factor that makes the difference. Under this point, we should design an experiment to verify this conjecture. Then, two sets of experiments are carried out. One experiment will use the SST images, with the coastal waters, as the evaluation database, and another experiment will use images without coastal waters, for comparison.

To evaluate the influence of different resolution on the model performance and to find out the better way to upsample ocean front, two sets of comparison experiments will be conducted, based on four representative databases. The first set of experiments makes use of the High-resolution and Low-resolution SST databases, and is conducted to display the effect of the resolutions of low-resolution images on the super-resolution performance. To make sure that the only variable is the resolution, we set the location, model, upsampling factor, and the number of training samples the same. The second set uses different kinds of input images to identify the best way to obtain high-resolution ocean-front image. One type of the input is SST images, selected from the Ocean SST database, another type of input is ocean-front images, selected from the SST ocean-front database. To evaluate their effect on ocean-front super-resolution, we use the ocean-front images rather than the SST images in the evaluation. Besides, we also control the variables in this set of experiments.

4.2 Evaluation Methods

We evaluate the model performance in terms of PSNR and Perceptual Loss, with upsampling factor set at 3. The equation of PSNR is defined as follows:

$$PSNR = 10 \times \log_{10}\left(\frac{1}{\sum_{i=1}^{n} \frac{\left|I(i)-\widehat{I}(i)\right|^2}{n}}\right) \tag{1}$$

where $I(i)$ and $\widehat{I}(i)$ denote the i^{th} pixel of the ground-truth SST image and the output image, respectively, and n is the number of pixels in the images. The pixel-wise losses between the reconstructed and the ground-truth images are averaged to evaluate the reconstruction quality.

In addition to PSNR, we further analyze the reconstruction quality with the Perceptual Loss. The Perceptual Loss is defined as follows:

$$L_X = \frac{1}{\mathbf{W_{i,j}} \mathbf{H_{i,j}}} \sum_{x=1}^{\mathbf{W_{i,j}}} \sum_{y=1}^{\mathbf{H_{i,j}}} (\phi_{i,j}(\mathbf{I^G})_{x,y} - (\phi_{i,j}(M(\mathbf{I^B}))_{x,y})^2 \tag{2}$$

where the model M is trained for the super-resolution task. $\mathbf{I^B}$ represents the input obtained upsampling with the bicubic method, and is compared with the corresponding ground-truth $\mathbf{I^G}$. $\phi_{i,j}$ represents the feature maps extracted from a convolutional layer, whose layer depths are indexed as i and j. All the convolutional layers are chosen from the VGG19 network, which is pretrained on the ImageNet database [16]. We extract feature maps using $VGG_{3,3}$ convolutional layers. $\mathbf{W_{i,j}}$ and $\mathbf{H_{i,j}}$ represent the height and width of the feature maps. Note that deeper convolutional layer extracts more abstract features [17–19]. The perceptual loss function pays attention to the content and overall spatial structure of the input images [18], rather than the texture and exact shape, while the PSNR is just the opposite.

We evaluate the PSNR and Perceptual Loss for the models trained on the 291 and China Ocean SST databases. For the China Ocean SST database, the coastal waters (keep the coastline) and the marine waters (delete the coastline) are tested respectively.

5 Analysis on the Experiment Results

Finally, Tables 1 and 2 tabulate the performance of the different models on the China Ocean SST images. As shown in Table 1, the modified model trained on the 291 database has a higher PSNR and Perceptual Loss than VDSR and bicubic methods, while the same model trained on the China Ocean SST database gains a slightly higher PSNR value, but a much lower Perceptual Loss. This proves the existence of data distribution difference. Then, Table 2 reveals the key factor that causes the difference. The results show a significant difference in the PSNR and Perceptual Loss achieved by the different models trained on different databases. Thus, the fact that the coastal waters make the data distribution of SST images different from standard images can be proved.

Table 1. The PSNR and Perceptual Loss of the different methods on the 291 and China Ocean SST database with coastline removed.

METHOD	PSNR	PERCEPTUAL LOSS
BICUBIC(291)	36.83	5.34
VDSR(291)	45.68	**3.05**
MODIFIED VDSR(291)	46.29	6.92
MODIFIED VDSR(SST)	**46.94**	3.79

Table 2. The PSNR and Perceptual Loss of the different methods on the China Ocean SST database.

METHOD	PSNR	PERCEPTUAL LOSS
BICUBIC	17.04	21.07
VDSR (SST)	17.67	53.77
MODIFIED VDSR (SST)	**21.53**	**5.89**

Table 3. The VDSR network trained on the 291 database, the down-sample factor set at 3

PSNR	BICUBIC	VDSR
LOW RESOLUTION	33.52	**36.06**
HIGH RESOLUTION	32.67	**38.25**

Figure 4 displays a SST image, captured on 1st January 2011, from the high-resolution Ocean SST database. The ground-truth image is first downsampled by 3 times, using the bicubic method, and then upsampled using the bicubic and the VDSR methods. It is hard for humans to figure out which method performs better from the output images. Therefore, we present the loss images. It is easy to tell that the loss between the VDSR output and the ground-truth image is smaller than that between the bicubic output and the ground-truth image. In other words, the VDSR model performs better than the bicubic method. We not only apply the VDSR model on high-resolution SST images, but also apply it to low-resolution images. The results are tabulated in Table 3.

As shown in Table 3, the VDSR model performs better than the bicubic method on both the high-resolution and low-resolution SST images, especially

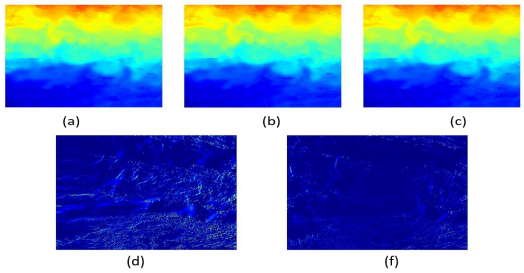

Fig. 4. Super-resolution effect using different methods on SST images. (a) An image from the high-resolution SST database, labeled as the ground-truth image (data domain 0-5000) (b) Its bicubic up-sampled image (c) The output image of the VDSR model (d) The loss between the ground-truth image and the bicubic image (data domain 0-30) (e) the loss between the ground-truth image and the model output image

Table 4. The EDSR model trained on the Ocean SST databases, the down-sample factor set at 3

PSNR	BICUBIC	EDSR
LOW RESOLUTION	33.52	**39.19**
HIGH RESOLUTION	32.67	**39.86**

Table 5. The models trained on the Ocean SST and SST ocean-front databases.

PSNR	SST	OCEAN-FRONT
BICUBIC	43.15	27.40
EDSR	31.85	34.55
VDSR	45.89	**34.78**
MODIFIED VDSR	**46.04**	34.77

on the high-resolution SST images. The reason for this can be that the high-resolution images contain more textures and sharper edges, which are hard for the bicubic method to reconstruct.

For comparison, we also apply EDSR, trained with the same databases. However, as presented in Table 4, the results are complicated. On the one hand, the performance of EDSR, in terms of PSNR, is $5.67dB$ and $7.19dB$ higher than that of the bicubic method, on the low-resolution and high-resolution SST images, respectively. These relative improvement is higher than that of VDSR, whose performance is $2.54dB$ and $5.58dB$ higher than bicubic, on the two datasets.

As shown in Figure 5, we choose the first image of the database to demonstrate the performance of the different methods on upsampling ocean front on SST images and SST ocean-front images. In our experiment, we choose the biggest 10% Singular Exponent (SE) pixels as the ocean front. From Figure 5 (b) to (g), we can hardly judge the best and the worst methods. Therefore, we present the loss images from Figure 5 (h) to (m). It can be seen from these images that the bicubic method achieves the worst performance on the SST ocean-front images, while VDSR achieves the best performance, with the SST images as input. The performances, in terms of PSNR, are presented in Table 5.

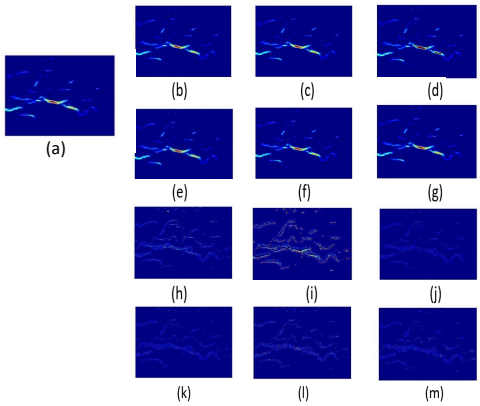

Fig. 5. Super-resolution effect using different methods on ocean front images. (a) The ground-truth image is chosen from the SST ocean-front database (data domain 100-350) (b) The bicubic up-sampled ocean-front image on the Ocean SST database (c) The bicubic up-sampled ocean-front image on the SST ocean-front database (d) The output ocean-front image of VDSR, trained on the Ocean SST database (e) The output ocean-front image of VDSR trained on the SST ocean-front database (f) The output ocean-front image from EDSR, trained on the Ocean SST database (g) The output ocean-front image of EDSR on the SST ocean-front database (h-m) Loss images between a ground-truth image and the output image, based on the bicubic, VDSR, EDSR methods on the Ocean SST database and SST ocean-front database respectively (data domain 0-30)

Table 5 shows the experiment results based on the different methods for upsampling SST ocean-front images from the Ocean SST database and the SST ocean-front database. In this set of experiments, we use MMF to calculate the ocean fronts from the SST images. We set the downsampling scale at 3, for both the Ocean SST database and the SST ocean-front database. Then, these images are sent to the networks to obtain the upsampled SST images and upsampled ocean-front images. After that, on the one hand, we extract ocean fronts from the upsampled SST image using MMF. Comparing with the ground-truth ocean-

front images, which are also calculated by using MMF, the modified VDSR achieves the best performance for the SST ocean-front super-resolution task in terms of PSNR, which is 46.07. On the other hand, the output ocean-front images of the different methods are compared with the ground-truth ocean-front images. It can be easily observed that the best performance is achieved by the VDSR method. Although EDSR takes downsampled images as the input, and it has better performance on standard databases, its domain adaption ability is worse than the VDSR network. The results reveal that the best way to reconstruct ocean front is to upsample the SST image rather than the ocean-front image. The reason for this may be that the ocean-front images are sparser than the SST image, which makes it harder to reconstruct features from the down-sampled ocean-front images.

6 Future Work and Conclusion

This paper points out the impact of the data distribution difference on the robustness of some deep learning models and also draws an interesting conclusion that the data distribution of SST and standard images differs the most in the ocean areas, rather than the sea-land intersection areas. Besides, we also propose a data transformation method, which can help to handle data from different databases, such as SST images and standard images. This work may be useful for further investigating new deep learning networks for super-resolution in geophysical fields, especially for zooming in sea surface features in remote sensing images. What's more, we propose four databases for two sets of experiments, which may promote oceanography community to validate their method and ameliorate networks for super-resolution task on remote sensing images. The experiment results prove that our data transformation method can not only improve the performance on the SST images, with different resolutions and locations, but also can improve the performance on standard images.

In the future, we will train a super-resolution network, based on the Low-resolution Ocean SST database, and take the High-resolution Ocean SST database as the ground-truth data. Then, we will also evaluate its performance on the Ocean SST database and SST ocean-front database. We believe that the future work will be more challenging and meaningful.

7 acknowledgments

This work was jointly supported by the National Natural Science Foundation of China (No. U1706218, 61971388, 62072287).

References

1. Yuting, Y., Junyu, D., Xin, S., Redouane, L., Muwei, J., Xinhua, W.: Ocean front detection from instant remote sensing SST images. IEEE Geoscience and Remote Sensing Letters **13**(12), 1960–1964 (2016)

2. Yuting, Y., Junyu, D., Xin, S., Estanislau, L., Quanquan, M., Xinhua, W.: A cfcc-lstm model for sea surface temperature prediction. IEEE Geoscience and Remote Sensing Letters **15**(2), 207–211 (2018)
3. Estanislau, L., Xin, S., Junyu, D., Hui, W., Yuting, Y., Lipeng, L.: Learning and transferring convolutional neural network knowledge to ocean front recognition. IEEE Geoscience and Remote Sensing Letters **14**(3), 354–358 (2017)
4. Estanislau, L., Xin, S., Yuting, Y., Junyu, D.: Application of deep convolutional neural networks for ocean front recognition. Journal of Applied Remote Sensing **11**(4), 042610 (2017)
5. Yuting, Y., Junyu, Kin-Man, L., Xin, S., Junyu, D., Hanjiang, L.: An Efficient Algorithm for Ocean-Front Evolution Trend Recognition. Remote Sensing **14**(2), 259 (2022)
6. Yuting, Y., Lam, K. M., Junyu, D., Xin, S., Jian, M.: Super-resolution on remote sensing images. In: Proceedings of the International Workshop on Advanced Image Technology, pp. 1–5. SPIE, Online (2021)
7. Yuting, Y., Lam, K. M., Junyu, D., Xin, S., Jian, M.: Application of GoogLeNet for Ocean-Front Tracking. In: Proceedings of the International Workshop on Advanced Image Technology, pp. 1–5. SPIE, Hong Kong, China (2022)
8. Oriol, P., Antonio, T., Hussein, Y.: Singularity analysis of digital signals through the evaluation of their unpredictable point manifold. International Journal of Computer Mathematics **90**(8), 1693–1707 (2013)
9. Aurélien, D., Ronan, F. Deep learning for ocean remote sensing: an application of convolutional neural networks for super-resolution on satellite-derived SST data. In: 9th IAPR Workshop on Pattern Recogniton in Remote Sensing (PRRS), pp. 1–6. IEEE, Cancun, Mexico (2016)
10. Chao, D., Chen Change, L., Kaiming H., Xiaoou, T.: Image super-resolution using deep convolutional networks. IEEE transactions on pattern analysis and machine intelligence **38**(2), 295–307 (2016)
11. Jiwon, K., Jung Kwon, L., Kyoung Mu, L.: Accurate image super-resolution using very deep convolutional networks. In: Proceedings of the IEEE conference on computer vision and pattern recognition (CVPR), pp. 1646–1654, IEEE, Las Vegas, Nevada, USA (2016)
12. Bee, L., Sanghyun, S., Heewon, K., Seungjun, N., Kyoung Mu, L.: Enhanced deep residual networks for single image super-resolution. In: Proceedings of the IEEE conference on Computer Vision and Pattern Recognition (CVPR), pp. 136–144, IEEE, Florida, USA (2017)
13. Marco, B., Aline, R., Christine, G., Marie, l., Alberi M.: Low-complexity single-image super-resolution based on nonnegative neighbor embedding. In: Proceedings of the British Machine Vision Conference, pp. 135.1–135.10, BMVA Press, Surrey, England (2012)
14. Yu-Heng, T., Mao-Lin, S., Sen, J., David E, D., Chia-Ping, C. Validation of the kuroshio current system in the dual-domain pacific ocean model framework. Progress in oceanography, **105**, 102–124 (2012)
15. II, L., Chun-Chieh, W., Iam-Fei, P., Dong-Shan, K. Upper-ocean thermal structure and the western north pacific category 5 typhoons. part I: Ocean features and the category 5 typhoons intensification. Monthly Weather Review **136**(9), 3288–3306 (2008)
16. Jia, D., Wei, D., Richard, S., Li-Jia, L., Kai, L., Fei-Fei, L.: Imagenet: A large-scale hierarchical image database. In: 2009 IEEE conference on computer vision and pattern recognition (CVPR), pp. 248–255, IEEE, Florida, USA (2009)

17. Matthew D, Z., Rob, F.: Visualizing and understanding convolutional networks. In: European conference on computer vision (ECCV), pp.818–833, Springer, Zurich, Switzerland (2014)
18. Christian, L., Lucas, T., Ferenc, H., Jose, C., Andrew, C., Alejandro, A., Andrew, A., Alykhan, T., Johannes, T., Zehan, W., et al.: Photo-realistic single image super-resolution using a generative adversarial network. In: Proceedings of the IEEE conference on computer vision and pattern recognition (CVPR), pp. 4681–4690, IEEE, Florida, USA (2017)
19. Junyu, D., Ruiying, Y., Xin, S., Qiong, L., Yuting, Y., Xukun, Q. Inpainting of remote sensing sst images with deep convolutional generative adversarial network. IEEE Geoscience and Remote Sensing Letters, **16**(2), 173–177 (2019)
20. Leo H, H.: Waves in oceanic and coastal waters. Cambridge university press, Cambridge, England (2010)